

Electrochemical Investigations of Biologically Active 1-(3-Hydroxy-2-pyridyl)-4,4,6-trimethyl-3,4-dihydropyrimidine-2[1*H*]-thione at Pyrolytic Graphite Electrode

Rajendra N. Goyal,* Sham M. Sondhi, and Anand M. Lahoti

Department of Chemistry, Indian Institute of Technology Roorkee, Roorkee-247 667, India

Received September 16, 2005; E-mail: rngcyfcy@iitr.ernet.in

Electrochemical behavior of a biologically active pyridinylpyrimidine derivative, 1-(3-hydroxy-2-pyridyl)-4,4,6-trimethyl-3,4-dihydropyrimidine-2[1*H*]-thione (**1**) has been investigated in aqueous phosphate buffers (1.9–10.6) at a pyrolytic graphite electrode (PGE). The oxidation occurred in a single well-defined oxidation peak, I_a, in the pH range 1.9–10.6. In the pH range 4.9–10.6, a reduction peak, II_c, was noticed in the reverse sweep that formed a quasi-reversible couple with peak II_a observed in the subsequent sweep towards positive potentials. The effect of concentration and sweep rate on peak potential and peak current of peak I_a established adsorption of **1** at the surface of PGE. Controlled potential coulometry experiments revealed the $5e^-$ oxidation of **1** in acidic solution and $7e^-$ oxidation in a neutral solution by an EC mechanism. UV–vis spectral and kinetic studies suggested formation of different intermediates in acidic and neutral media. The major product of oxidation at pH 2.7 was characterized as 2,2,4-trimethyl-2*H*-9-oxa-10-thia-1,4a,5-triazaphenanthrene 10,10-dioxide (**6**). At physiological pH 7.1, 1-(2,5-dioxo-6-pyridyl)-4,4,6-trimethyl-1,4-dihydropyrimidine-2-thiol (**7a**) and 1-(3,6-dioxo-3,6-dihydro-2-pyridyl)-4,4,6-trimethyl-1,4-dihydropyrimidine-2-sulfonic acid (**10**) were identified as the oxidation products by GC-MS. A mechanism for the electrooxidation of **1** at PGE has also been suggested.

Pyridine and pyrimidine derivatives are well-known in medicinal chemistry for their therapeutic applications.[1,2] Synthesis of new pyridine and pyrimidine derivatives has enormous interest in heterocyclic chemistry since they also serve as key intermediates in the synthesis of a variety of polyaryl strands such as pyridylpyrimidine compounds.[3,4] Recently, a U.S. patent[5] revealed anti-cancer activity of pyridylpyrimidine derivatives. A literature survey indicated that physical properties such as the crystal structure of pyridylpyrimidine derivatives have been extensively studied in the past.[6] However, no attempts have been made to study the electrochemical behavior of this important class of compounds.

Electrochemical investigations of pyridine and pyrimidine based sulfa drugs provide major challenges both from mechanistic and analytical view point.[5,7,8] In contrast to conditions of conventional oxidation using a variety of oxidizing agents like H_2O_2, aqueous iodine, dimethyldioxirane, etc., electrooxidation employs conditions close to physiological systems.[9–11] For the last several years, our laboratory has been keenly involved in studying the redox behavior of the biologically significant compounds viz. purines, pyrimidines and their nucleosides, nucleotides, etc.[12,13] It has been revealed from these studies that redox investigations provide unique and invaluable information on the mechanism of degradation of various biologically important organic compounds.[14–16] Hence, it was considered worthwhile to synthesize the pyridylpyrimidine derivative, 1-(3-hydroxy-2-pyridyl)-4,4,6-trimethyl-3,4-dihydropyrimidine-2[1*H*]-thione (**1**) (Scheme 1) as a promising anti-inflammatory/analgesic compound and to study its electrochemical behavior at the pyrolytic graphite electrode (PGE).

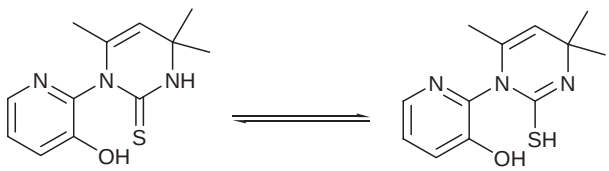

1

Scheme 1.

The investigations were carried out in an aqueous phosphate buffer supporting electrolytes in a wide pH range, by using linear and cyclic sweep voltammetry, controlled potential coulometry, and UV–vis spectral studies, and the products of electrode reaction were characterized by using various spectroscopic techniques.

Experimental

Instrumentation. Melting points (mp) were obtained on a capillary apparatus and remain uncorrected. Infrared spectra were recorded using a Perkin-Elmer 1600 FT spectrophotometer and only characteristic peaks are reported. ^{1}H NMR spectra were measured in deuterated solvents ($CDCl_3$, DMSO-d_6, and D_2O) with TMS as an internal standard by using a Bruker AC-300F, NMR spectrometer. FAB-MS spectrum was reordered on a JEOL SX-102 (FAB) mass spectrometer. Linear and cyclic sweep voltammetric studies were carried out by using a Cypress (Model CS-1090) electroanalytical system. Controlled potential coulometry experiments were performed by using BASi Epsilon-EC-Ver. 1.50.69_XP and BASi CV-50 W (Model MF-9093) potentiostats. UV–vis spectral changes and kinetic studies were monitored

Published on the web April 7, 2006; DOI: 10.1246/bcsj.79.569

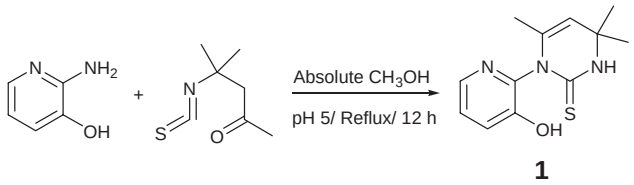

1

Scheme 2.

in a 1 cm quartz cell by using a Perkin-Elmer Lambda 35 UV–vis spectrophotometer. Gas chromatography-mass spectrometry (GC-MS) was performed with a Perkin-Elmer model Clarus-500 mass spectrometer.

Compound **1** was synthesized in the laboratory by the one-pot reaction of 2-amino-3-hydroxypyridine (0.220 g, 2 mmol) and 4-isothiocyanato-4-methyl-2-pentanone[17] (0.314 g, 2 mmol) as reported earlier (Scheme 2).[18]

Electrochemical Studies. A stock solution of compound **1** (2.0 mM) was prepared using doubly distilled water. Phosphate buffers of different pH having an ionic strength of 1.0 M were prepared[19] from analytical grade chemicals (NaH_2PO_4 and Na_2HPO_4) (Merck). Conventional electrochemical equipment[20] were used to carry out voltammetric studies. PGE (surface area; ≈2.2 mm^2) was fabricated in laboratory by a reported method.[21] The surface of PGE was renewed after recording each voltammogram by rubbing it with emery paper (C/P-400) and then cleaning the surface with a jet of water, followed by gentle drying with tissue paper. The surface area of the electrode changed each time due to rubbing, and hence the peak current values showed a variation of ±10%. Thus, voltammetric measurements were performed in triplicate and an average value of the current is reported. All potentials were referred to a Ag|AgCl electrode at an ambient temperature of 25 ± 2 °C. Controlled potential coulometry experiments were carried out in a single compartment cell equipped with a three-electrode system containing a pyrolytic graphite plate (6 × 1.5 cm^2) as working, cylindrical platinum gauze (1.5 × 15 cm^2) as auxiliary, and Ag|AgCl as reference electrodes, respectively.

For voltammetric experiments, 2.0 mL of the stock solution was mixed with 2.0 mL of phosphate buffer (μ = 1.0 M) of appropriate pH so that the effective ionic strength of the solution became 0.5 M. The solutions were deoxygenated by bubbling nitrogen gas for 8–10 min before recording the voltammograms. In controlled potential coulometry experiments, a potential ≈100 mV more positive than the oxidation peak potential was applied. The numbers of electrons, "*n*," involved in electrooxidation at pH 2.7 and 7.1 were determined by monitoring the decay of current with time.[22] The progress of electrolysis was monitored by withdrawing 2–3 mL of the sample from the working compartment of the H-cell at different time intervals and was transferred each time to a 1 cm quartz cell, and UV-spectrum was recorded in the wavelength region 215–360 nm. In another set of experiments when absorbance at λ_{max} reduced to ≈50%, the applied potential was turned off and spectral changes of the solution were monitored at different time intervals to determine the wavelength region in which the UV-absorbing intermediates were generated. The decay of absorbance with time was recorded at pre-selected wavelengths and the values of the rate constant (k) were calculated at different pH from the linear $\log(A - A_\infty)$ versus time plots.

For identification of the electrooxidation products, 10–15 mg of compound **1** was bulk electrolyzed in an H-cell. The reference arm of the H-cell was filled with buffer solution (pH 2.7 or 7.1), whereas the other arm had a solution of **1** at the same pH. The three-electrode system used was essentially the same as that used in the controlled potential coulometry experiment.[5] Electrolysis of the solution was carried out at a potential ≈100 mV more positive than the peak I_a potential. Nitrogen gas was continuously bubbled and the solution was constantly stirred using a magnetic stirrer during the course of electrolysis. Progress of electrolysis was monitored by recording cyclic voltammograms at different time intervals. When the oxidation peak (I_a) disappeared, the exhaustively electrolyzed solution was removed from the H-cell and lyophilized. The freeze-dried material obtained was extracted with methanol (AR grade, 2 × 10 mL), and the extract was concentrated and dried under reduced pressure. The dried sample was dissolved in methanol, 5 μL of the solution was injected for GC-MS analysis, and the spectrum was recorded in EI mode at 70 eV.

Results and Discussion

Voltammetric Behavior. Linear sweep voltammetry (LSV) of a 1.0 mM solution of **1** at a sweep rate 20 mV s^{-1} exhibited a well-defined oxidation peak I_a in the entire pH range (1.9 to 10.6). The peak potential of peak I_a was found to be dependent on pH and shifted to less positive potential with an increase in pH, indicating thereby the involvement of protons in the electrooxidation process.

In cyclic voltammetry (CV) at a sweep rate of 100 mV s^{-1} a well-defined oxidation peak I_a was observed in the entire pH range of 1.9–10.6 when the sweep was initiated in the positive direction. A typical cyclic voltammogram of compound **1** at pH 2.7 is depicted in Fig. 1A.

In the reverse sweep the reduction peak II_c was noticed in the pH range 4.9–10.6, which formed a quasi-reversible couple with peak II_a, observed in the subsequent sweep towards positive potential. The cyclic voltammogram of compound **1** at pH 7.1 clearly shows two oxidation peaks, I_a and II_a, and a reduction peak, II_c (Fig. 1B). The peak potential (E_p) of peaks I_a, II_c, and II_a were linearly dependent on pH as depicted in Fig. 2. The E_p versus pH relations and correlation coefficients for these peaks are presented in Table 1.

In a separate experiment, cyclic voltammograms of compound **1** were also recorded by initiating the sweep in the negative direction to know whether peak II_c is due to the reduction of species generated in the peak I_a reaction or to an independent reduction of compound **1**. In this experiment, peak II_c was not observed in the cyclic voltammograms; therefore, it was deduced that peak II_c is due to the reduction of the product of the peak I_a reaction.

The effect of the concentration of compound **1** on the peak current (i_p) of peak I_a was studied in the range of 0.55 to 3.50 mM at pH 2.7 and 7.1. The background current of the phosphate buffer was subtracted from the observed value of i_p. The dependence of peak current on concentration for peak I_a is shown in Fig. 3. It is clear from the plot that i_p increases linearly with increases in concentration until ≈2.0 mM, and at concentrations >2.0 mM attained almost a constant value. This behavior indicated that compound **1** adsorbs at the surface of PGE.[23]

The effect of sweep rate on peaks I_a, II_c, and II_a of compound **1** was studied in detail at pH 7.1 in the sweep range 10–800 mV s^{-1}. Figure 4 presents cyclic voltammograms recorded for compound **1** at different sweep rates. Sweep rates >800 mV s^{-1} could not be used because the oxidation peak

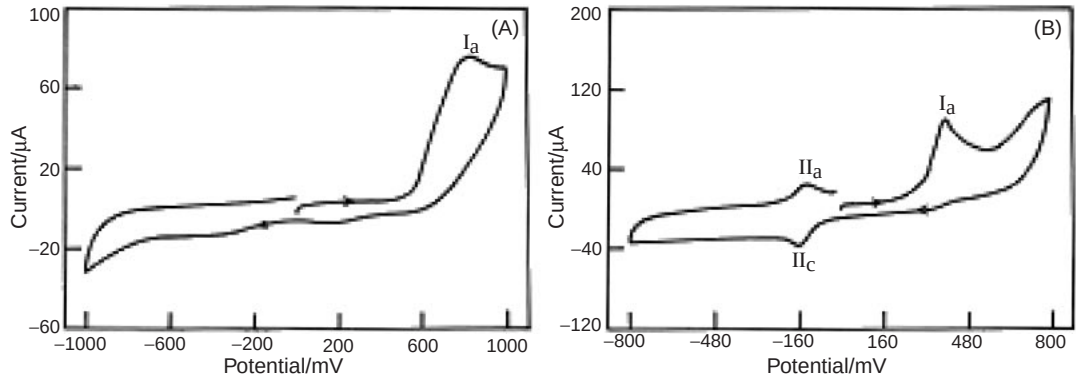

Fig. 1. Typical cyclic voltammograms of 1.0 mM **1** at PGE with sweep rate, 100 mV s^{-1} in phosphate buffer of (A) pH 2.7; (B) pH 7.1.

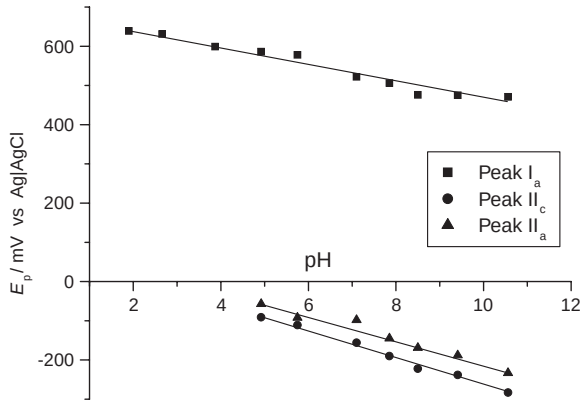

Fig. 2. Change in peak potentials (vs Ag|AgCl) at different pH for 1.0 mM **1** at PGE; sweep rate, 100 mV s^{-1}.

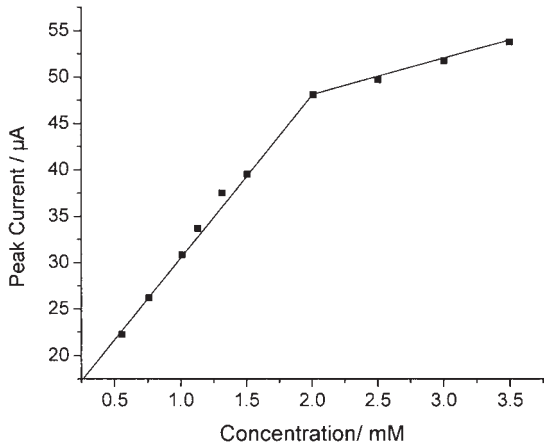

Fig. 3. Dependence of peak current (i_p) for peak I_a with increasing concentration of **1** at pH 2.7.

Table 1. Peak Potential (E_p) and pH Relation for Various Oxidation and Reduction Peaks Observed in Cyclic Voltammograms (Sweep Rate; 100 mV s^{-1}) of 1.0 mM **1**

Peak	pH range	E_p and pH relation (vs Ag|AgCl)	Correlation coefficient
I_a	1.9–10.6	$E_p = (688 - 22.2\text{pH})$ mV	0.9639
II_c	4.9–10.6	$E_p = (84.9 - 34.9\text{pH})$ mV	0.9923
II_a	4.9–10.6	$E_p = (95.4 - 30.5\text{pH})$ mV	0.9663

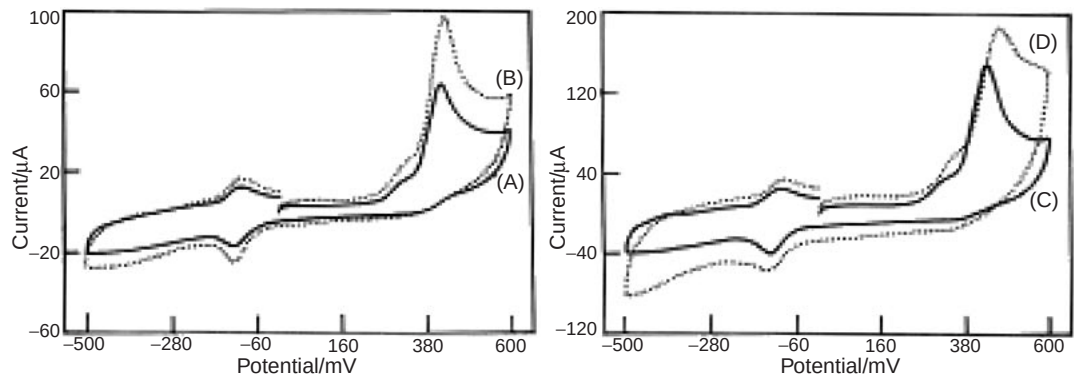

Fig. 4. Comparison of cyclic voltammograms of 1.0 mM **1** at pH 7.1 at sweep rate (A) 75, (B) 125, (C) 175, and (D) 600 mV s^{-1}.

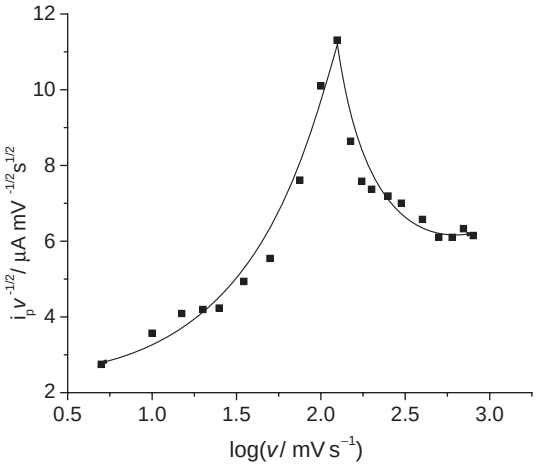

Fig. 5. Observed variation of peak current function ($i_p v^{-1/2}$) for peak I_a with the logarithm of sweep rate ($\log v$) for 1.0 mM **1** at pH 7.1.

I_a merged with the background. The E_p value of peak I_a was found to shift 5 mV per ten fold increase in sweep rate range (10–250 mV s^{-1}), whereas the shift increases to 10 mV at higher sweep rates. The peak current for peak I_a increases linearly with increases in sweep rate. The ratio of peak currents (i_{IIa}/i_{IIc}), however, remained practically constant (≈0.9) with increases in sweep rate in the range 50–800 mV s^{-1}. This behavior supported the quasi-reversible nature of the redox couple. The plot of the peak current of peak I_a versus $\log v$ showed a break at around $\log v = 2.1$. Thus, at a sweep rate of ≈125 mV s^{-1}, the mechanism of electrooxidation of **1** appeared to change from diffusion controlled to complications due to adsorption as shown in Fig. 5.

In controlled potential coulometry experiments, the numbers of electrons (n) involved in the electrooxidation of **1** at different pH were calculated from the graphical integration of the current–time curve. The plots of $\log i_p$ vs time were linear for the first 25–30 min of electrolysis and thereafter deviation from the straight line was noticed. This deviation clearly indicated that for the first ≈30 min the electrode reaction followed a simple path and thereafter-subsequent chemical reactions played an important role. A similar observation has also been reported by Cauquis and Parker[24] for an electrochemical reaction followed by irreversible chemical reactions, i.e., an EC mechanism. The average experimental values of n at pH 2.7 and 7.1 were 5.20 ± 0.20 and 7.10 ± 0.18, respectively, per mole of compound **1**.

UV–Vis Spectral Studies. Spectral changes observed during the electrooxidation of compound **1** are shown in Figs. 6A and 6B. At pH 2.7, a 0.05 mM solution of **1** exhibited two well-defined absorption bands at $\lambda_{max} = 240$ and 315 nm, which are represented by curve "a" in Fig. 6A. Upon application of a potential (≈100 mV more positive than peak I_a potential), absorbance in the region 230–250 and 280–360 nm systematically decreased, while absorbance in the region 250–280 nm systematically increased. Curve "i" (Fig. 6A) was recorded at 180 min of electrolysis, and it was observed that bands at 240 and 315 nm completely diminished. No clear isosbestic point was noticed during the spectral changes at pH 2.7.

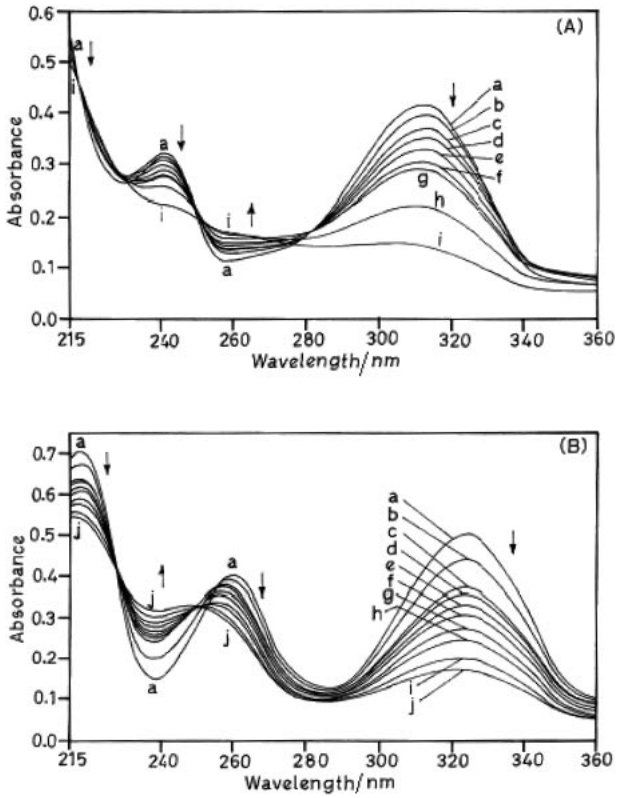

Fig. 6. Spectral changes observed during electrolysis of 0.05 mM **1** at PGE, **[A]** at pH 2.7, curves were recorded at (a) 0, (b) 5, (c) 15, (d) 30, (e) 45, (f) 60, (g) 90, (h) 120, and (i) 180 min of electrolysis; **[B]** at pH 7.1, curves were recorded at (a) 0, (b) 10, (c) 20, (d) 30, (e) 45, (f) 60, (g) 90, (h) 120, (i) 160, and (j) 180 min of electrolysis.

At pH 7.1, a 0.05 mM solution of **1** exhibited three well-defined absorption bands at $\lambda_{max} = 218$, 260, and 325 nm. Upon application of a potential (≈100 mV more positive than that of peak I_a), absorbance in the region 215–230 and 250–360 nm systematically decreased, while absorbance in the region 230–250 nm systematically increased. After 180 min of electrolysis (curve "j" in Fig. 6B), it was found that bands at 218, 260, and 325 nm were completely diminished. In this case a clear isosbestic point was noticed at 230 nm. The isosbestic point observed during electrolysis at pH 7.1 indicates that the intermediates formed during electrooxidation and the starting material have the same absorbance at 230 nm.

In a different set of experiments, after electrolyzing the solution of **1** for 80 min (when λ_{max} reaches ≈50%), the potentiostat was open circuited and UV spectra were recorded at different time intervals. It was observed that absorbance in the region 215–320 nm continued to decrease due to the decay of the intermediate generated during the electrooxidation of **1**. Thus, a UV-absorbing electro-active intermediate is generated and decayed due to involvement of subsequent chemical reactions. The kinetics of decay of the UV-absorbing intermediate were monitored by recording absorbance at selected wavelengths against time. The time vs absorbance profile recorded after turning off the potential showed an exponential decay (Fig. 7) and the plots of $\log(A - A_\infty)$ vs time at different wavelengths were linear, as shown in the Fig. 7 inset

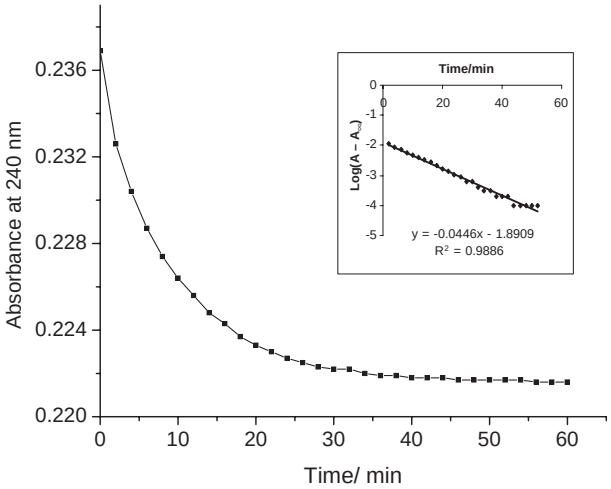

Fig. 7. Plot of absorbance vs time and $\log(A - A_\infty)$ vs time (inset) for decay of UV-absorbing electro-active intermediate generated during electrooxidation of 0.05 mM **1** at pH 2.7. The time on X-axis is after open circuit relaxation.

Table 2. Pseudo-First-Order Rate Constants Calculated for the Decay of UV-Absorbing Intermediate Generated during Electrooxidation of 0.05 mM Solution of Compound **1**

pH	λ/nm	$k^{a)}/\times 10^{-3}\,s^{-1}$
2.7	240	1.71
	265	1.59
	315	1.65
7.1	240	1.10
	260	1.05
	320	1.11

a) Average of at least two replicate determinations.

(where A_∞ and A are the absorbance at infinite time and at reaction time, respectively). The values of the rate constant (k) were calculated from the slope value of the linear best fit equation for the $\log(A - A_\infty)$ vs time plots at different pH; the wavelengths are summarized in Table 2. It is observed that the k values are nearly 1.5 times higher at pH 2.7 in comparison to pH 7.1, and suggested that the electron-transfer mechanism at pH 2.7 and 7.1 involve different intermediates.

Products Characterization. Electrooxidation products of compound **1** were characterized by GC-MS studies. This analytical technique has been found useful in characterizing the electrooxidation products of various biomolecules.[25] The GC-MS spectrum of lyophilized product obtained at pH 2.7 exhibited only one major peak at R_t 20.14 min having a molecular ion peak at m/z 280 ($M^+ + 1$, 10%). The other high mass peaks observed in the fragmentation pattern are summarized in Table 3. Based on mass calculations, the compound was identified as 2,2,4-trimethyl-2*H*-9-oxa-10-thia-1,4a,5-triazaphenanthrene 10,10-dioxide (**6**). At physiological pH 7.1, the oxidized sample gave two major peaks at R_t 19.64 and 19.70 min in the gas chromatogram. The compound eluted under peak R_t 19.64 in MS gave m/z 264 ($M^+ + 1$, 15%), and it was identified as 1-(2,5-dioxo-6-pyridyl)-4,4,6-trimethyl-1,4-dihydropyrimidine-2-thiol (**7a**). The second peak at R_t 19.70 on mass analysis gave m/z 312 ($M^+ + 1$, 5%), and it was characterized as 1-(3,6-dioxo-2-pyridyl)-4,4,6-trimethyl-1,4-dihydropyrimidine-2-sulfonic acid (**10**). The molar mass and relative abundance of high mass peaks observed in GC-MS of these products are presented in Table 3.

Table 3. Molar Masses and Relative Abundance of High Mass Peaks Observed in the Fragmentation Pattern of the Products of Oxidation of Compound **1**

pH	Product	R_t/min	($M^+ + 1$) peak	High molar mass peaks
2.7	**6**	20.14	280	253 (100%); 223 (65%); 166 (5%); 119 (8%)
7.1	**7a**	19.64	264	222 (12%); 221 (55%) 204 (28%); 147 (57%); 73 (100%)
	10	19.70	312	286 (5%); 254 (12%); 204 (90%); 191 (8%); 133 (20%)

Attempts for the separation of the products **7a** and **10** to further characterize them by various spectroscopic techniques were unsuccessful due to their very close retention times in GC. Nevertheless, the dark brown solid **6** (mp 260 °C decomp.) obtained at pH 2.7 was further characterized by IR and NMR. The FT-IR spectrum of **6** exhibited major peaks at (KBr, ν_{max}): 3186, 2926 (C–H), 1642 (C=N), 1594, 1502 (C=C), 1399, 1321 (O=S=O), 1283 cm^{-1}. The ^1H NMR spectrum of **6** showed signals at (D_2O, 300 MHz) δ 1.67 (s, 3H, $-CH_3$), 1.72 (s, 3H, $-CH_3$), 1.94 (s, 3H, $-CH_3$), 4.79 (s, 1H, olefinic), 6.98–7.03 (dd, 1H, Ar–H, $J = 2.0$ and 6.9 Hz), 7.25–7.28 (d, 1H, Ar–H, $J = 7.7$ Hz), 7.76–7.77 ppm (d, 1H, Ar–H, $J = 7.6$ Hz) and confirmed the structure as 2,2,4-trimethyl-2*H*-9-oxa-10-thia-1,4a,5-triazaphenanthrene 10,10-dioxide (**6**).

Electrooxidation Mechanism. The oxidation products identified in acidic and neutral media for compound **1** suggest that the electron-transfer mechanisms involved at pH 2.7 and 7.1 are different. The voltammetric and controlled potential coulometric results revealed that electrooxidation of **1** occurs in an overall $5H^+$, $5e^-$ oxidation at pH 2.7 and $7H^+$, $7e^-$ oxidation at pH 7.1, respectively (per mole). Thus, a tentative electrooxidation mechanism (Scheme 3) can be suggested on the basis of the experimental results.

Compound **1**, being a 2-thioxopyrimidine, derivative can exist in two tautomeric forms, **1a** and **1b**. It has been revealed that a thione–thiol equilibrium shifts to the thione in polar solvents such as water, ethanol, etc.,[26] but, in strongly acidic conditions the reverse is true.[27] At pH 2.7, $1H^+$, $1e^-$ oxidation of **1a** gives rise to the free radical **2a** at the electrode surface. A $1e^-$, $1H^+$ oxidation of various thiols has been well-reported in the literature[28] and it has also been established that the removal of a proton occurs from the –SH group. Combination of two moles of the radical **2a** will rapidly give the S–S linked dimer **3**. The disulfides are expected to be sufficiently stable, however, the hydrolysis of such compounds in acidic and neutral media is well-reported.[29] In attempt to further confirm the formation of disulfide **3**, a limited quantity of electrical charge ($1 \times 96500\,C\,mol^{-1}$) was passed in a solution of **1**. Such an electrolysis resulted in the formation of the starting materials

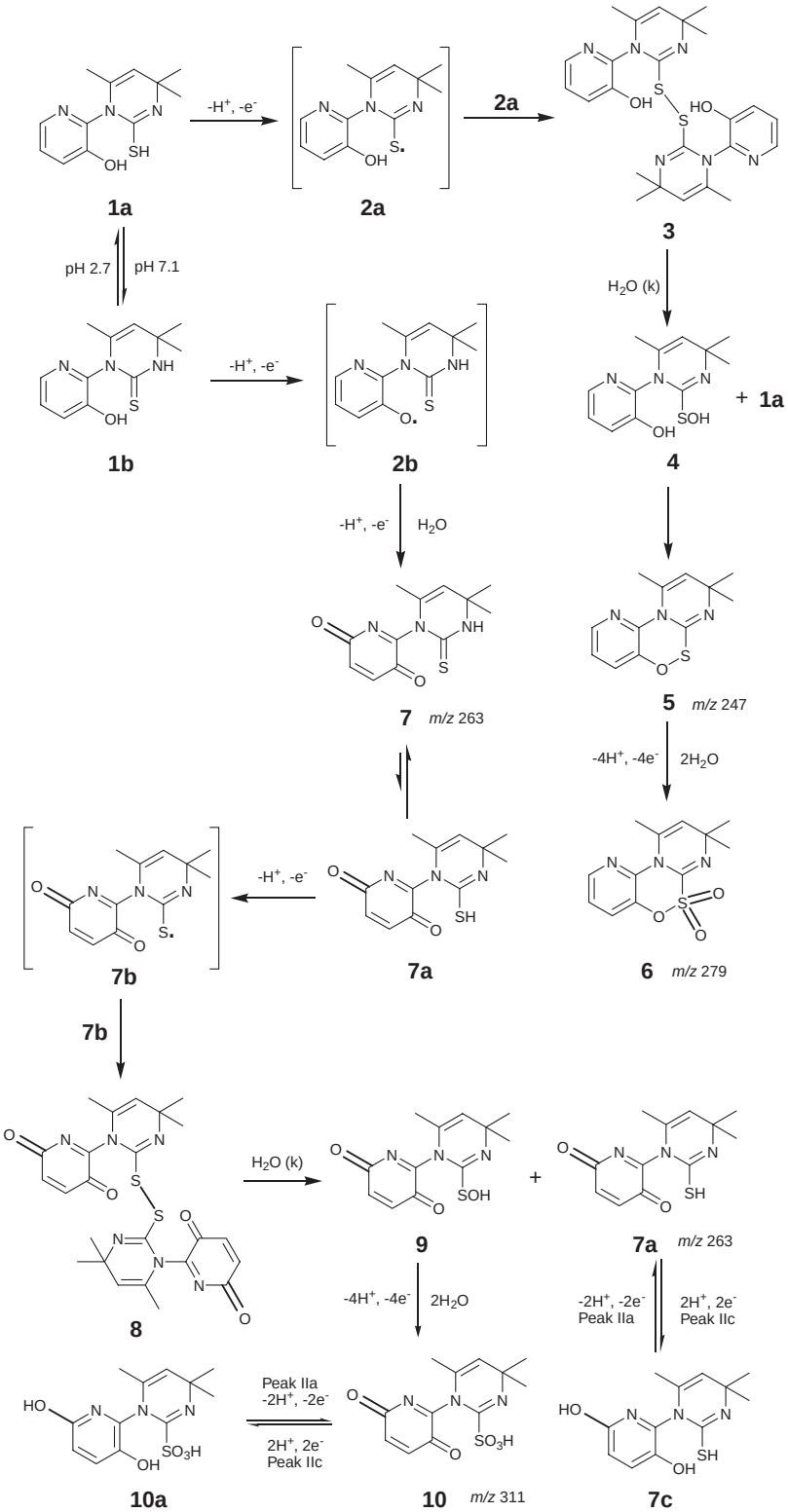

Scheme 3. Tentative electrooxidation mechanism explaining formation of different products of **1** at pH 2.7 and 7.1.

1 and **5** (m/z 247) as confirmed by the molar masses in the GC-MS. Thus, the disulfide **3** appeared to undergo hydrolysis and the hydrolysis seemed to play an important role at this stage. The attack of water molecules at the S–S linkage rapidly gives compound **4** and the starting material **1**. This addition of a water molecule to compound **3** is the rate determining step and occurs in a pseudo-first-order reaction having the rate constant $k = \approx 1.65 \times 10^{-3}\ s^{-1}$, to give **4**.

The sulfonic acid derivatives are known for high reactivity[30] and hence, **4** can easily convert to the chemically stable compound **5** by the elimination of a water molecule such an elimination will cause cyclization to yield the stable six-member

ring compound **5**. Such dehydration and cyclization in an acidic/basic medium and also during electrochemical transformations are well-known in the literature.[31] Compound **5** then further undergoes oxidation in $4H^+$, $4e^-$ processes to yield the dioxythia-derivative **6** as the final product. The formation of compounds having an O=S=O group as the stable oxidation product during the oxidation of thio-compounds is well documented in the literature.[32,33]

On the other hand, at pH 7.1, compound **1** seems to exist predominantly in the form **1b** and hence $1H^+$, $1e^-$ oxidation will give rise to the free radical **2b** at the surface of PGE. Further $1H^+$, $1e^-$ oxidation of **2b** in the presence of water gives the stable dione **7**. To further confirm the formation of **7** from **1a**, a fixed amount of charge ($2 \times 96500\,C\,mol^{-1}$) was passed in a solution of **1a**. The product obtained in lyophilization followed by GC-MS analysis exhibited a peak at m/z 264 (R_t 17.85 min). Thus, it is clear that $2H^+$, $2e^-$ oxidation of **1** gives compound **7**.

The pseudo-first-order rate constant values (k) determined at pH 7.1 indicate that the chemical follow-up step is also involved at this pH. Hence, it is expected that the electron-transfer mechanism at this pH also involves an intermediate similar to **3**. This can be explained on the basis of thione–thiol equilibrium between **7** and **7a**. Although the equilibrium is favorable towards thione **7**, the thiol form **7a** also exists at the electrode surface.[26] Hence, $1H^+$, $1e^-$ oxidation of **7a** will give **7b**, which on combination of similar species will give the disulfide **8**. The compound **8** can hydrolyze in a simple chemical reaction to give two products, the sulfenic acid derivative **9** and dione **7a**. Thus, the dione **7a** was identified as one of the major oxidations product at pH 7.1. The other product, **10**, identified in the GC-MS at pH 7.1, is the $4H^+$, $4e^-$ oxidation product of the reactive sulfenic acid derivative **9**. The diones **7a** and **10** have a *p*-benzoquinone-type moiety and hence both of them would easily reduce in a reversible $2H^+$, $2e^-$ process to yield the corresponding diols **7c** and **10a**, respectively. One would expect that two redox couples should be noticed corresponding to these reduction/oxidation, however, only one redox couple was observed. At higher concentrations of **1** ($\approx$1.5 mM), the redox couple showed a tendency to split into two couples. Thus, it appears that the E_p of theses couples is very close due to the almost similar structures of **7a** and **10**, and hence a single redox couple is observed in the CV. The suggested mechanism explains all the observed voltammetric, coulometric, and spectral data. However, it must be realized that the mechanism described in Scheme 3 for the formation of **6**, **7a**, and **10** is one of the several pathways possible at the surface of PGE.

In conclusion, the present studies establish that electron-transfer reactions and the oxidation mechanisms of 1-(3-hydroxy-2-pyridyl)-4,4,6-trimethyl-3,4-dihydropyrimidine-2[1*H*]-thione (**1**) are rather complex. Nevertheless, voltammetric, UV–vis spectral, controlled potential coulometry, and various spectroscopic methods were found very useful to reveal such a complex electron-transfer mechanism. The present studies reveal the metabolic route of the biologically significant organic compound **1** and provide useful information to develop its novel derivatives as prospective anti-inflammatory/analgesic compounds.

One of the authors (AML) is thankful to the Indian Institute of Technology Roorkee (IITR) for the award of an Institute Fellowship, sponsored by the Ministry of Human Resource Development (MHRD) through IITR grant code MHR 02/23/200/304. The authors are grateful to SAIF-PU Chandigarh and RSIC-CDRI Lucknow for permitting the use of ^{1}H NMR and FAB-MS analyses, respectively.

References

1 S. A. Laufer, G. K. Wagner, *J. Med. Chem.* **2002**, *45*, 2733.
2 S. M. Sondhi, S. Rajvanshi, N. Singh, S. Jain, A. M. Lahoti, *Cent. Eur. J. Chem.* **2004**, *2*, 141.
3 R. Kramer, I. O. Fritsky, *Eur. J. Org. Chem.* **2000**, 3505.
4 N. Nishiwaki, K. Yamashita, M. Azuma, T. Adachi, M. Tamura, M. Ariga, *Synthesis* **2004**, 1996.
5 K. Amala, B. Rao, A. K. Sathya, V. C. Nannapaneni, S. Rachakonda, PCT Int. Appl. WO 2004108699 A1 20041216, **2004**.
6 M. L. Glowka, H. Foks, C. Orlewska, *J. Chem. Crystallogr.* **1994**, *24*, 375.
7 N. C. Mathur, R. N. Goyal, W. U. Malik, *Bull. Soc. Chim. Fr.* **1990**, *127*, 353.
8 R. N. Goyal, A. Mittal, *Anal. Chim. Acta* **1990**, *228*, 273.
9 C. Prado, G. Flechsig, P. Gruendler, J. Foord, S. John, F. Marken, R. G. Compton, *Analyst* **2002**, *127*, 329.
10 S. Peressini, C. Tavagnacco, G. Costa, C. Amatore, *J. Electroanal. Chem.* **2002**, *532*, 295.
11 A. M. Oliveira-Brett, J. A. P. Piedade, L. A. Silva, V. C. Diculescu, *Anal. Biochem.* **2004**, *332*, 321.
12 R. N. Goyal, N. Jain, D. K. Garg, *Bioelectrochem. Bioenerg.* **1997**, *43*, 105.
13 R. N. Goyal, P. P. Thankachan, N. Jain, *Bull. Chem. Soc. Jpn.* **2000**, *73*, 1515.
14 G. Dryhurst, *Chem. Rev.* **1990**, *90*, 795.
15 M. Z. Wrona, R. N. Goyal, D. J. Turk, C. L. Blank, G. Dryhurst, *J. Neurochem.* **1992**, *59*, 1392.
16 R. N. Goyal, A. Kumar, P. Gupta, *J. Chem. Soc., Perkin. Trans. 2* **2001**, 618.
17 H. Singh, S. Kumar, *J. Chem. Soc., Perkin. Trans. 1* **1987**, 261.
18 S. M. Sondhi, R. N. Goyal, A. M. Lahoti, N. Singh, R. Shukla, R. Raghubir, *Bioorg. Med. Chem.* **2005**, *13*, 3185.
19 G. D. Christian, W. C. Purdy, *J. Electroanal. Chem.* **1962**, *3*, 363.
20 R. N. Goyal, G. Dryhurst, *J. Electroanal. Chem.* **1982**, *135*, 75.
21 G. Dryhurst, D. L. McAlliser, *Laboratory Techniques in Electroanalytical Chemistry*, ed. by P. T. Kissinger, W. R. Heineman, Marcel Dekker, New York, **1984**, p. 264.
22 J. J. Lingane, *Electroanalytical Chemistry*, 2nd ed., Wiley Interscience, New York, **1966**, p. 222.
23 R. S. Nicholson, I. Shain, *Anal. Chem.* **1964**, *36*, 706.
24 G. Cauquis, V. D. Parker, *Organic Electrochemistry*, ed. by M. M. Baizer, Marcel Dekker, New York, **1973**, p. 134.
25 R. N. Goyal, S. M. Sondhi, A. M. Lahoti, *New J. Chem.* **2005**, *29*, 587.
26 S. Stoyanov, I. Petkov, L. Antonov, T. Stoyanova, *Can. J. Chem.* **1990**, *68*, 1482.
27 M. J. Nowak, H. Rostkowska, L. Lapinski, J. Leszczyoski, J. S. Kwiazkoski, *Spectrochim. Acta, Part A* **1991**, *47*, 339.
28 N. Berthe-Gaujac, I. Demachy, Y. Jean, F. Volatron,

Chem. Phys. Lett. **1994**, *22*, 145.
29 S. Patai, *The Chemistry of the Thiol Group, Part 2*, John Wiley & Sons, **1974**, pp. 788–792.
30 C. Bontempelli, F. Mafno, G. A. Mazzocchin, *J. Electroanal. Chem.* **1973**, *42*, 57.
31 D. Nematollahi, Z. Forooghi, *Tetrahedron* **2002**, *58*, 4949.
32 A. B. Penenory, J. E. Argüello, M. Puiatti, *Eur. J. Org. Chem.* **2005**, 114.
33 R. N. Goyal, S. M. Sondhi, A. M. Lahoti, A. A. Abdulla, *Indian J. Chem., Sect. A* **2005**, *44*, 463.